A THREE DIMENSIONAL PRIMITIVE EQUATION MODEL FOR APPLICATION TO MESOSCALE ATMOSPHERIC PHENOMENA

by

Jack T. Norton, Jr.

United States
Naval Postgraduate School

THESIS

A THREE DIMENSIONAL PRIMITIVE
EQUATION MODEL FOR APPLICATION TO
MESOSCALE ATMOSPHERIC PHENOMENA

by

Jack T. Norton, Jr.

This document has been approved for public release and sale; its distribution is unlimited.

T136459

LIBRARY
NAVAL POSTGRADUATE SCHOOL
MONTEREY, CALIF. 93940

A Three Dimensional Primitive Equation Model for Application to Mesoscale Atmospheric Phenomena

by

Jack Trask Norton, Jr.
Lieutenant Commander, United States Navy
B.S., Oregon State University, 1962

Submitted in partial fulfillment of the
requirements for the degree of

MASTER OF SCIENCE IN METEOROLOGY

from the
NAVAL POSTGRADUATE SCHOOL
September 1970

RARY
AL POSTGRADUATE SCHOOL
TEREY, CALIF. 93940

ABSTRACT

A three dimensional primitive equation model based on the Boussinesq equations is developed and applied to the mesoscale. The model is tested with one dimensional flow in a balanced state and with two cases of gravity waves, which are forecast for 30 minutes and compared with the analytic solutions.

TABLE OF CONTENTS

LIST OF FIGURES

LIST OF SYMBOLS AND ABBREVIATIONS

c	Phase speed of disturbance (m sec^{-1}).
c_p	Specific heat of air at constant pressure (joule gm^{-1} $^oK^{-1}$).
f	Coriolis parameter (sec^{-1}).
f_o	Constant coriolis parameter (.8365 x 10^{-4} sec^{-1}).
F	Forcing function for the relaxation equation.
g	Acceleration due to gravity (m sec^{-2}).
i	Grid index in x direction.
IM	Number of grid points in the x direction.
j	Grid index in y direction.
JM	Number of grid points in the y direction.
k	Grid index in z direction.
KM	Number of grid points in the z direction.
λ	Wave number in the x direction = $2\pi/L_x$.
L_x	Wave length in the x direction.
L_y	Wave length in the y direction.
L_z	Wave length in the z direction.
m	Wave number in the z direction = π/L_z.
n	Growth rate of disturbance (sec^{-1}).
P	Pressure (mb).
P_o	1000 (mb).
R	Gas constant for air (joule gm^{-1} $^oK^{-1}$).
t	Time (sec).
T	Temperature (^oK).

u x component of horizontal velocity (m sec^{-1}).

v y component of horizontal velocity (m sec^{-1}).

$\vec{V}_3$ Three dimensional wind vector.

w Vertical component of velocity (m sec^{-1}).

W Scale value of vertical motion.

Δx Mesh length in the x direction.

Δy Mesh length in the y direction.

Δz Mesh length in the z direction.

ζ Vertical component of relative vorticity (sec^{-1}).

θ Deviation from adiabatic potential temperature (^{o}K).

θ_o 300 (^{o}K).

$\bar{\theta}$ Stratification potential temperature (^{o}K).

Θ Potential temperature (^{o}K).

κ R/c_p.

μ Wave number in the y direction = π/L.

ν Kinematic viscosity coefficient (m sec^{-1}).

β Pressure parameter.

β_o Hydrostatic part of the pressure parameter.

β' Non-hydrostatic part of the pressure parameter.

ρ Density of air (kgm m^{-3}) .

∇ Del operator = $\vec{i}\frac{\partial}{\partial x} + \vec{j}\frac{\partial}{\partial y} + \vec{k}\frac{\partial}{\partial z}$.

∇_3^2 Laplacian operator = $\frac{\partial^2}{\partial x^2} + \frac{\partial^2}{\partial y^2} + \frac{\partial^2}{\partial z^2}$.

∇_3 Finite difference form of the del operator.

ACKNOWLEDGMENT

The author extends his gratitude to Dr. R. L. Alberty, whose suggestion it was to undertake this project, and whose unfailing optimism and infinite patience contributed a great deal to its completion. Thanks also go to Dr. R. T. Williams for his excellent guidance in dynamic and finite differencing matters, and for providing the means for testing the model. Time for the numerical integrations was provided by the W. R. Church Computer Center at the Naval Postgraduate School.

I. INTRODUCTION

Several recent attempts to understand the complex dynamic interaction of the thunderstorm and its environment have been made using the dynamical thunderstorm model presented by Newton and Newton (1959). The model proposes that strong vertical drafts within the thunderstorm create an effective barrier to the environmental flow. The analysis by Browning (1964) concerning airflow near and within severe thunderstorms provides valuable additional knowledge about the character of the vertical motion. Convective storm mass and water budget assessments such as the one conducted by Newton (1966) substantiate the concept of upper level entrainment of cool, dry air first recognized by Normand (1946).

Radar determined chaff trajectories were used successfully by Fankhauser (1968) to follow the motion of air parcels in and around a thunderstorm. Further use of chaff will undoubtedly make possible a good understanding of the paths taken by environmental parcels from all positions around a local storm.

As noted by Lilly (1962), the evolution of convective motions with relatively large amplitudes can best be described through the combined application of conventional analytic methods and numerical experimentation. Ogura (1963) discussed the possible use of the primitive equations as a basis for forecasting small scale dynamical features. He

suggested that interaction between convective elements and the prevailing wind field could thus be investigated numerically. The results of such efforts, correlated with the subjective modeling, should produce verifying as well as augmenting information for the subjective products.

A numerical study of turbulent flow conducted by Deardorff (1970) makes use of a three dimensional primitive equation model. The forecast procedure he uses is similar to the procedure used in this study.

The numerical model presented here is a three dimensional primitive equation model based on the Boussinesq equations. Forecasts are made for the wind components and potential temperature after imposing initial conditions on these same parameters.

The grid used for computations is 25 by 25 in the horizontal, with 15 levels in the vertical. Grid interval in all directions is 1 kilometer. A mean latitude of 35^{o} is used to determine the Coriolis parameter, which is treated as a constant.

Predictions are made using the IBM OS/360 computer of the W. R. Church computer center. A one minute time step was chosen to conform to computational stability requirements.

II. DEVELOPMENT OF THE MODEL

A. THE FORECAST EQUATIONS

The pressure term in the equation of motion may be expressed as

$$\frac{1}{\rho} \nabla_3 P = \frac{RT}{P} \nabla_3 \left[\frac{P_o}{C_p^{1/K}} \beta^{1/K} \right]$$

$$= \Theta \nabla_3 \beta ,$$

where

$$\beta = C_p \left[\frac{P}{P_o} \right]^K$$

and

$$\Theta = T \left[\frac{P_o}{P} \right]^K .$$

Using this result in the component equations of motion yields

$$\frac{du}{dt} = - \Theta \frac{\partial \beta}{\partial x} + fv + \nu \nabla_3^2 u, \tag{1}$$

$$\frac{dv}{dt} = - \Theta \frac{\partial \beta}{\partial y} - fu + \nu \nabla_3^2 v, \tag{2}$$

$$\frac{dw}{dt} = - \Theta \frac{\partial \beta}{\partial z} - g + \nu \nabla_3^2 w. \tag{3}$$

Forming the perturbation expressions

$$\beta = \beta_o(z) + \beta'(x,y,z,t)$$

and

$$\Theta = \beta_o + \theta(x,y,z,t)$$

where

$$|\beta'| \ll \beta_o \quad \text{and} \quad |\theta| \ll \theta_o ,$$

and substituting into (1) yields

$$\frac{du}{dt} = -\theta_o \frac{\partial \beta'}{\partial x} + fv + \nu \nabla_3^2 u , \tag{4}$$

where the relatively small product $\theta \frac{\partial \beta'}{\partial x}$ is neglected.

Similarly,

$$\frac{dv}{dt} = -\theta_o \frac{\partial \beta'}{\partial y} - fu + \nu \nabla_3^2 v. \tag{5}$$

For the vertical component equation the substitution yields

$$\frac{dw}{dt} = -\theta_o \frac{\partial \beta_o}{\partial z} - \theta_o \frac{\partial \beta'}{\partial z} - \theta \frac{\partial \beta_o}{\partial z} - g + \nu \nabla_3^2 w.$$

Since β_o and θ_o are related by the hydrostatic equation

$$\frac{\partial \beta_o}{\partial z} = -\frac{g}{\theta_o} ,$$

the vertical component equation may be written

$$\frac{dw}{dt} = -\theta_o \frac{\partial \beta'}{\partial z} + \frac{g\theta}{\theta_o} + \nu \nabla_3^2 w. \tag{6}$$

Defining $\phi = \theta_o \beta'$ and substituting into (4), (5) and (6) results in the system of equations

$$\frac{\partial u}{\partial t} = -\mathcal{L}(u) - \frac{\partial \phi}{\partial x} + fv + \nu \nabla_3^2 u \tag{7}$$

$$\frac{\partial v}{\partial t} = -\mathcal{L}(v) - \frac{\partial \phi}{\partial y} - fu + \nu \nabla_3^2 v \tag{8}$$

$$\frac{\partial w}{\partial t} = -\mathcal{L}(w) - \frac{\partial \phi}{\partial z} + \frac{g\theta}{\theta_o} + \nu \nabla_3^2 w \tag{9}$$

$$\frac{\partial \theta}{\partial t} = -\mathcal{L}(\theta) \tag{10}$$

$$\nabla_3 \cdot \bar{V}_3 = 0 \tag{11}$$

where $\mathcal{L}(S) = -\bar{V}_3 \cdot \nabla_3 S$, $S = u, v, w, \theta$. Equation (11) is the continuity equation. In order to eliminate sound waves, incompressible flow is assumed. Ogura and Phillips (1962) have shown that this system of equations, which they call the anelastic equations, is quite accurate for shallow convection.

B. DETERMINATION OF THE PRESSURE TERMS

Equations (7), (8), and (9) may be combined and written in the vector form

$$\frac{\partial \vec{V}_3}{\partial t} = -(\vec{V}_3 \cdot \nabla_3)\vec{V}_3 - \nabla_3 \phi - f(\vec{k} \times \vec{V}_3) + \frac{g\theta}{\theta_o}\vec{k} + \nu \nabla_3^2 \bar{V}_3 . \tag{12}$$

Taking the three dimensional divergence of (12) yields

$$\frac{\partial}{\partial t}(\nabla_3 \cdot \vec{V}_3) = 0$$

$$= -\nabla_3 \cdot \left[(\vec{V}_3 \cdot \nabla_3)\,\vec{V}_3\right] - \nabla_3^2\phi$$

$$- \nabla_3 \cdot \left[f(\vec{k} \times \vec{V}_3)\right] + \frac{g}{\theta_o}\frac{\partial \theta}{\partial z} \qquad (13)$$

For a limited horizontal scale the Coriolis parameter may be treated as constant. Thus, (13) becomes

$$\nabla_3^2\phi = \nabla_3 \cdot \left[(\vec{V}_3 \cdot \nabla_3)\vec{V}_3\right] - f_o\,\nabla_3 \cdot (\vec{k} \times \vec{V}_3) + \frac{g}{\theta_o}\frac{\partial \theta}{\partial z}$$

$$= -\nabla_3 \cdot \left[(\vec{V}_3 \cdot \nabla_3)\,\vec{V}_3\right] + f_o\,\zeta + \frac{g}{\theta_o}\frac{\partial \theta}{\partial z}\,, \qquad (14)$$

which can be solved using relaxation techniques.

III. FINITE DIFFERENCING

Equations (7) through (10) are solved numerically by introducing finite differences in x, y, z and t. Solution for the pressure term can be carried out by applying the extrapolated Liebmann relaxation technique to evaluate (14). Appendix A shows the development of the relaxation equation. The procedure used to compute the forcing function is included in Appendix B.

In order to maintain finite differencing consistency throughout the entire forecast process, it is necessary to use the finite difference forms of equations (7), (8) and (9) to form the finite difference equivalent of equation (14).

The vertical domain consists of fifteen levels with values of u, v, w, θ, and ϕ assigned to each grid point. The space differencing method used is based on a scheme devised by Arakawa (1966) and is designed to conserve total energy. The non-linear operator, $\mathfrak{L}(S)$, takes the finite difference form

$$\mathfrak{L}(S) = \Big[(u_{i+1,j,k} + u_{i,j,k})\ (S_{i+1,j,k} + S_{i,j,k}) - (u_{i-1,j,k} + u_{i,j,k})\ (S_{i-1,j,k} + S_{i,j,k})\Big]/4\,\Delta x + \Big[(v_{i,j+1,k} + v_{i,j,k})\ (S_{i,j+1,k} + S_{i,j,k}) - (v_{i,j-1,k} + v_{i,j,k})\ (S_{i,j-1,k} + S_{i,j,k})\Big]/4\,\Delta y$$

$$+ \left[(w_{i,j,k+1} + w_{i,j,k})\ (S_{i,j,k+1} + S_{i,j,k})\right.$$

$$\left. - (w_{i,j,k-1} + w_{i,j,k})\ (S_{i,j,k-1} + S_{i,j,k})\right] \quad /4\,\Delta z.$$

The linear space derivatives are of the centered form

$$\frac{\partial S}{\partial x} = \frac{(S_{i+1,j,k} - S_{i-1,j,k})}{2\,\Delta x} .$$

Centered time differencing is used for all forecasts except the first which employs a forward time step.

IV. BOUNDARY CONDITIONS

The boundary conditions are selected to enforce mass and energy conservation within the domain of the grid. Figure 1 illustrates the grid domain and boundary placement in the horizontal. Boundaries in the vertical are similarly placed, with bottom and top boundaries at

$$k = \frac{2 + 3}{2} = 2.5$$

and

$$k = \frac{(KM-1) + (KM-2)}{2}$$

respectively, where KM is the number of grid points in the vertical.

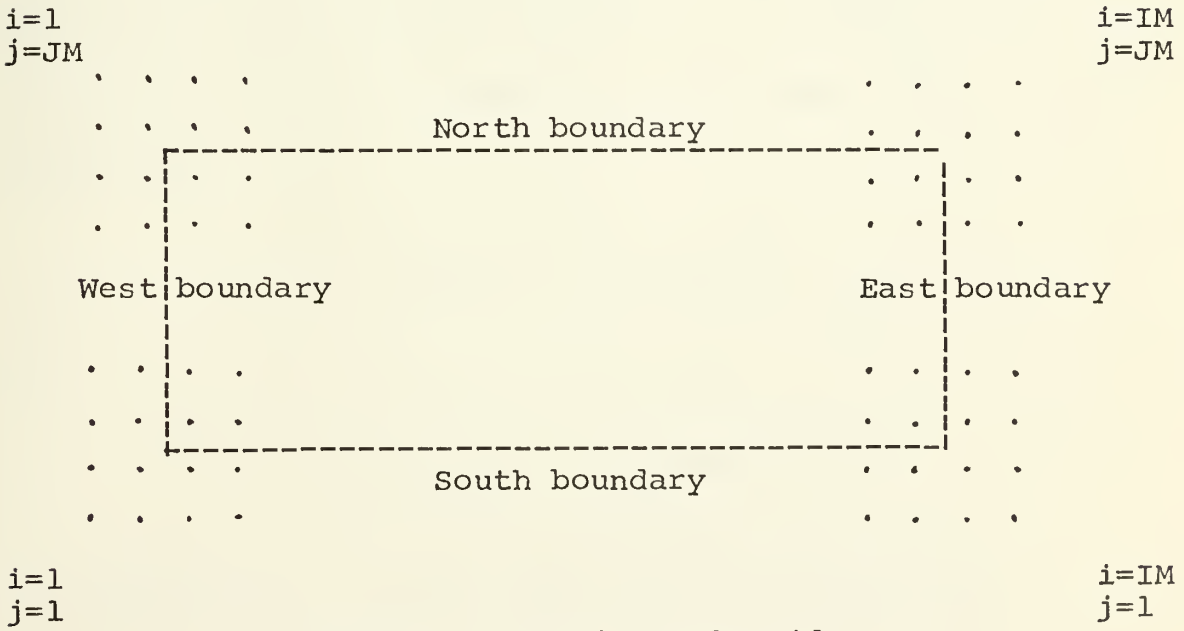

Figure 1: Horizontal grid

Periodicity in the east-west direction ensures cyclic continuity of all parameters. This condition is imposed by

applying the relationships

$$S_{1,j,k} = S_{IM-3,j,k} ,$$

$$S_{2,j,k} = S_{IM-2,j,k} ,$$

$$S_{IM-1,j,k} = S_{3,j,k} ,$$

and

$$S_{IM,j,k} = S_{4,j,k} ,$$

where S = u, v, w, θ and ϕ. Since values of S at points in the outer columns are required in solving for the pressure term and in calculating divergence, a four point periodicity constraint is necessary.

In order to prevent the flow of mass and energy through the northern and southern boundaries, a condition of no flux is imposed on the v component of the wind. This is accomplished by

$$v_{i,2,k} = -v_{i,3,k}$$

and

$$v_{i,JM-1,k} = -v_{i,JM-2,k} .$$

The values of v on the outer row are obtained by

$$v_{i,1,k} = v_{i,4,k}$$

and

$$v_{i,JM,K} = v_{i,JM-3,k} .$$

The u and w wind components and θ are projected outward by

$$S_{i,1,k} = S_{i,2,k} = S_{i,3,k}$$

and $$S_{i,JM,k} = S_{i,JM-1,k} = S_{i,JM-2,k} ,$$

where $S = u,w,\theta$.

Values of pressure on the outer rows are obtained by using the geostrophic relationship

$$\frac{\partial \Phi}{\partial y} = -fu .$$

The upper and lower boundaries are treated in the same manner as the north and south boundaries, with the no-flux condition being imposed on w by

$$w_{i,j,2} = -w_{i,j,3} ,$$

$$w_{i,j,KM-1} = -w_{i,j,KM-2} ,$$

$$w_{i,j,1} = w_{i,j,4} ,$$

and $$w_{i,j,KM} = w_{i,j,KM-3} .$$

Values of u and v on the top and bottom levels are obtained by

$$S_{i,j,1} = S_{i,j,2} = S_{i,j,3}$$

and

$$S_{i,j,KM} = S_{i,j,KM-1} = S_{i,j,KM-2} \quad ,$$

where $S = u, v$.

The hydrostatic relationship,

$$\frac{\partial \phi}{\partial z} = \frac{g\theta}{\theta_o} \quad ,$$

is used to determine values of θ and ϕ above the top and below the bottom boundaries. The application of proper boundary conditions was found to be critical. Appendices C and D show the development of these conditions in detail.

V. INITIAL CONDITIONS

Initialization of the u,v,w and θ fields was accomplished according to the experiment being prepared. During the check-out phase of programming the model, a steady-state, geostrophic, zonal flow was used to provide a check on computational stability. Subsequent tests were initialized to include gravity waves, both stable and unstable.

A. ZONAL FLOW CASE

Stability of the balanced state was tested by inserting a 10 m sec^{-1} wind throughout the u field. Initial v and w fields were set to zero. Standard atmospheric values of pressure were introduced and, by using an adiabatic lapse rate of temperature, the equation

$$\theta = T\left[\frac{P_o}{P}\right]^{k}$$

provided the initial θ field. Since the relaxation technique used to obtain the initial ϕ field proved to be extremely efficient, choosing the initial guess ϕ field as an arbitrary constant was convenient.

B. GRAVITY WAVE CASES

Linearized gravity wave solutions, accurate for small scale perturbations only, were used to test the model. For the stable gravity wave the following relationships describe the initial conditions.

$$u = -\frac{\lambda\, m\, W}{\lambda^2 + \mu^2} \sin \lambda x \cos \mu y \cos mz$$

$$v = -\frac{\mu\, m\, W}{\lambda^2 + \mu^2} \cos \lambda x \sin \mu y \cos mz$$

$$w = W \cos \lambda x \cos \mu y \sin mz$$

$$\theta = \frac{W}{\lambda c} \frac{\partial \bar{\theta}}{\partial z} \sin \lambda x \cos \mu y \sin mz \ .$$

Phase speed may be calculated from the relationship

$$c = \frac{N}{\lambda} \sqrt{\frac{\lambda^2 + \mu^2}{\lambda^2 + \mu^2 + m^2}} \qquad (15)$$

For the gravity wave associated with unstable stratification, the initializing relationships are

$$u = \frac{\lambda}{m} \left[1 + \frac{N^2}{n^2}\right] W \sin \lambda x \cos \mu y \cos mz$$

$$v = \frac{\mu}{m} \left[1 + \frac{N^2}{n^2}\right] W \cos \lambda x \sin \mu y \cos mz$$

$$w = W \cos \lambda x \cos \mu y \sin mz$$

$$\theta = -\frac{W}{n} \frac{\partial \bar{\theta}}{\partial z} \cos \lambda x \cos \mu y \sin mz \ ,$$

where

$$N^2 = \frac{g}{\theta_o} \frac{\partial \bar{\theta}}{\partial z}$$

and

$$n^2 = \frac{-N^2(\lambda^2 + \mu^2)}{\lambda^2 + \mu^2 + m^2} \quad , \tag{16}$$

where n is the growth rate of the disturbance.

The ϕ field may be initialized for the gravity waves exactly as in the zonal flow case.

VI. RESULTS

The balanced state introduced for the one dimensional flow case as a check on the computational stability and forecast capability of the model should remain indefinitely, subject to the validity of the approximations in the basic equations, round-off error in the computer, accuracy of the assumptions at the boundaries, and stability requirements. The use of proper boundary conditions was the most important factor in determining the length of the forecast produced. Until the combination of boundary conditions shown in section IV and Appendix C was utilized, the forecasts were valid for no longer than 5 minutes. Longest forecasts of the balanced flow were obtained by applying the boundary conditions that are periodic in x, geostrophic in y, and hydrostatic in z.

Accuracy of forecasts was monitored through the calculation of the three dimensional divergence, which should have remained very small throughout the prognosis. The smallest possible relaxation tolerance consistent with single precision mode capability of the computer was found to allow the least amount of divergence. When larger tolerances were allowed, a substantial amount of divergence developed on the north and south boundaries at mid-levels and increased with height.

A test was conducted to determine the optimum relaxation coefficient for the grid interval and grid domain which the

model employs. The value selected did not appear too critical, as long as it was between 1.5 and 1.7.

For the first experiment that produced a relatively long prognosis, an adiabatic lapse rate of temperature and standard atmospheric values of pressure were used to initialize the potential temperature field. This produced a slightly unstable average lapse rate of potential temperature, with two thin stable layers included near the bottom. With these conditions the model forecast for 47 minutes.

The time step was then decreased from 1 minute to 40 seconds, with the result that the forecast proceeded for 72 time steps, which was essentially the same length as the previous forecast. In an effort to improve the initial balance, pressure values which would lead to a nearly neutral lapse rate of potential temperature were inserted in the first experiment. The forecast continued for 56 minutes. Returning again to the conditions used in experiment one, the lapse rate of potential temperature was modified to include stable layers across the top and bottom boundaries. With these conditions the model produced a forecast for 69 minutes.

Introduction of a small perturbation in the form of a gravity wave provided another method of observing the model behavior. The gravity wave in stable stratification should propagate in the x direction only, without growing. With unstable stratification the wave should not propagate, and should grow at a rate given by equation (16).

The wave inserted for the stable case was forecast for 30 minutes, after which a comparison was made between the initial and forecast values of u, v, w and θ. With this comparison it was possible to observe the amount of spurious growth and the speed of propagation. The relationship of the initial and forecast wave forms in x for the line j=8, k=6 is shown in Figures 2a, 2b, 2c and 2d. The exact solution of equation (15) indicated that the phase speed for the case shown was 10.2 m sec^{-1}. Phase speeds calculated from the plotted values were 10.5 m sec^{-1}, 10.4 m sec^{-1}, 9.5 m sec^{-1} and 10.3 m sec^{-1} for u, v, w and θ respectively. The difference in phase speeds between w and θ was in no doubt related to the fact that the wave grew. The wave forms in y illustrated in Figures 3a, 3b, 3c and 3d show that the wave grew in the y direction but did not propagate. Figures 4a, 4b, 4c and 4d show that no propagation of the wave occurred in the z direction, but that the growth was not smooth.

For each combination of initial conditions applied to the wave, growth was apparent. By modifying the lapse rate of potential temperature toward adiabatic conditions, the growth decreased.

The gravity wave with unstable stratification was compared in the same manner as was the stable case. Figures 5a, 5b, 5c and 5d show that the wave did not propagate. Furthermore, the growth that was experienced by the wave was very close to that which was expected. The amplification

factor based on the computed growth rate of $.1376 \times 10^{-2}$ sec^{-1} was determined to be 11.9 at 30 minutes, and amplification factors of 11.8, 12.0, 12.4 and 11.3 were noted for u, v, w and θ respectively.

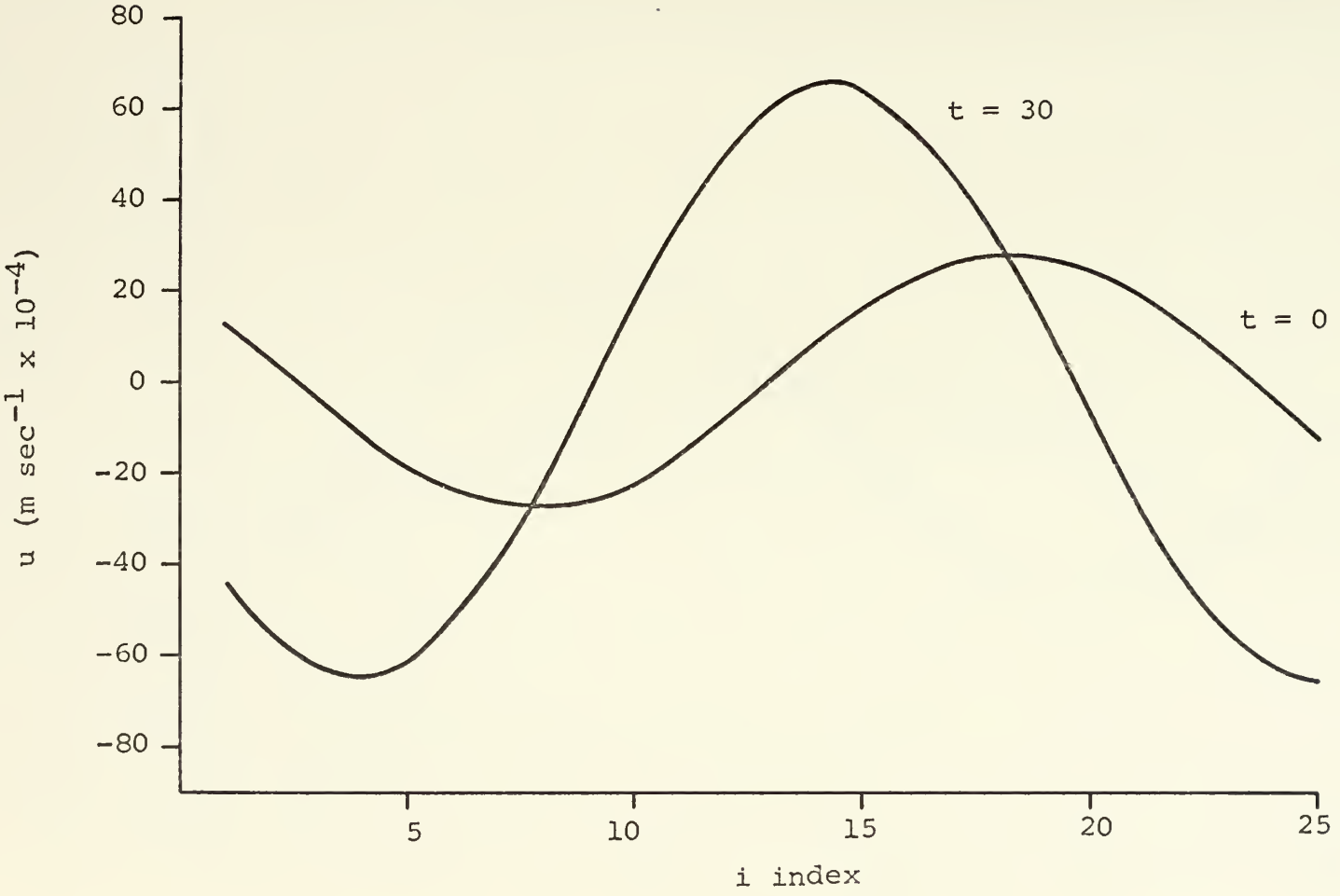

Fig. 2a - The u component of the wave form in the x direction for j=8, k=6, stable case

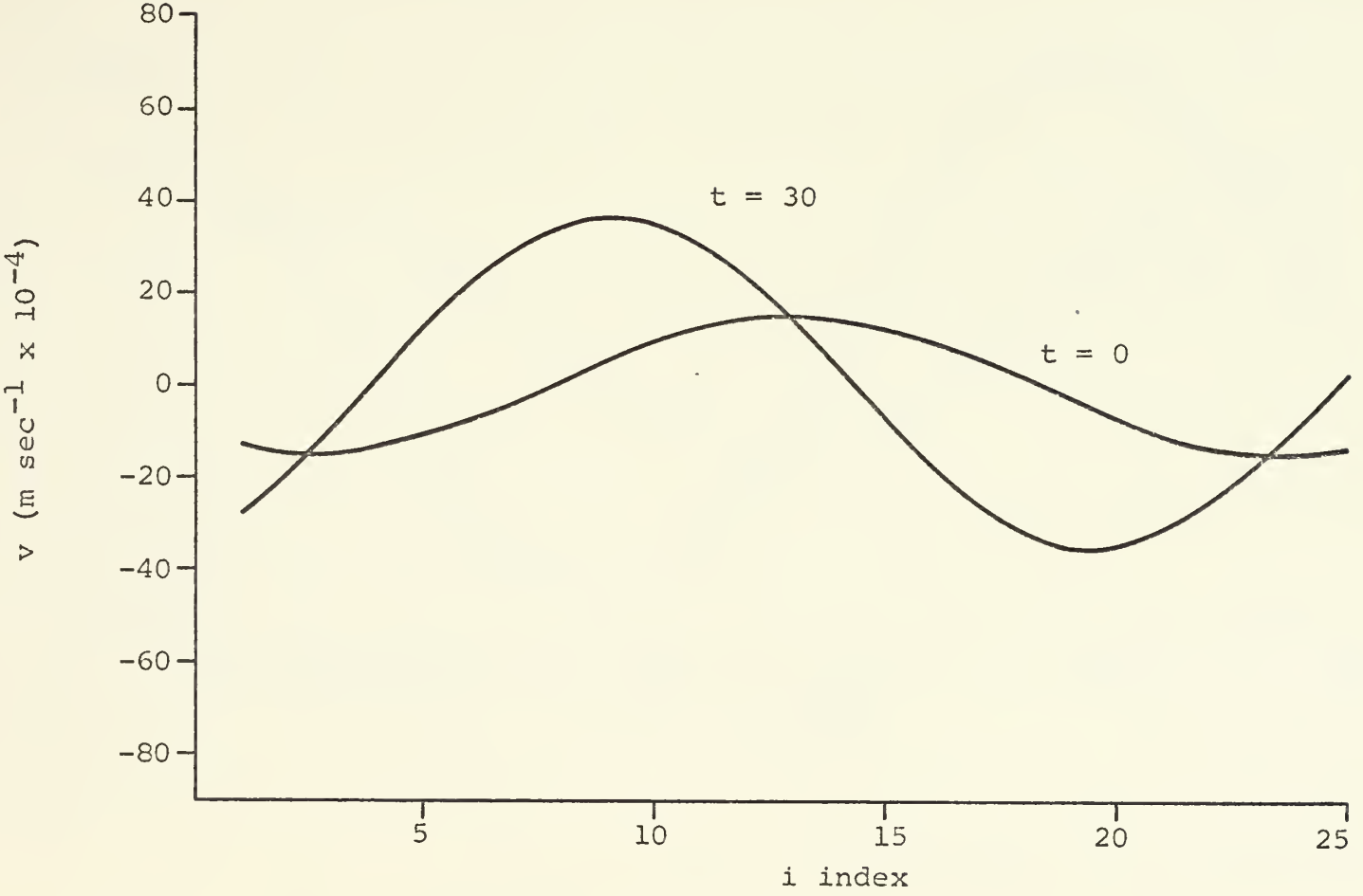

Fig. 2b - The v component of the wave form in the x direction for j=8, k=6, stable case

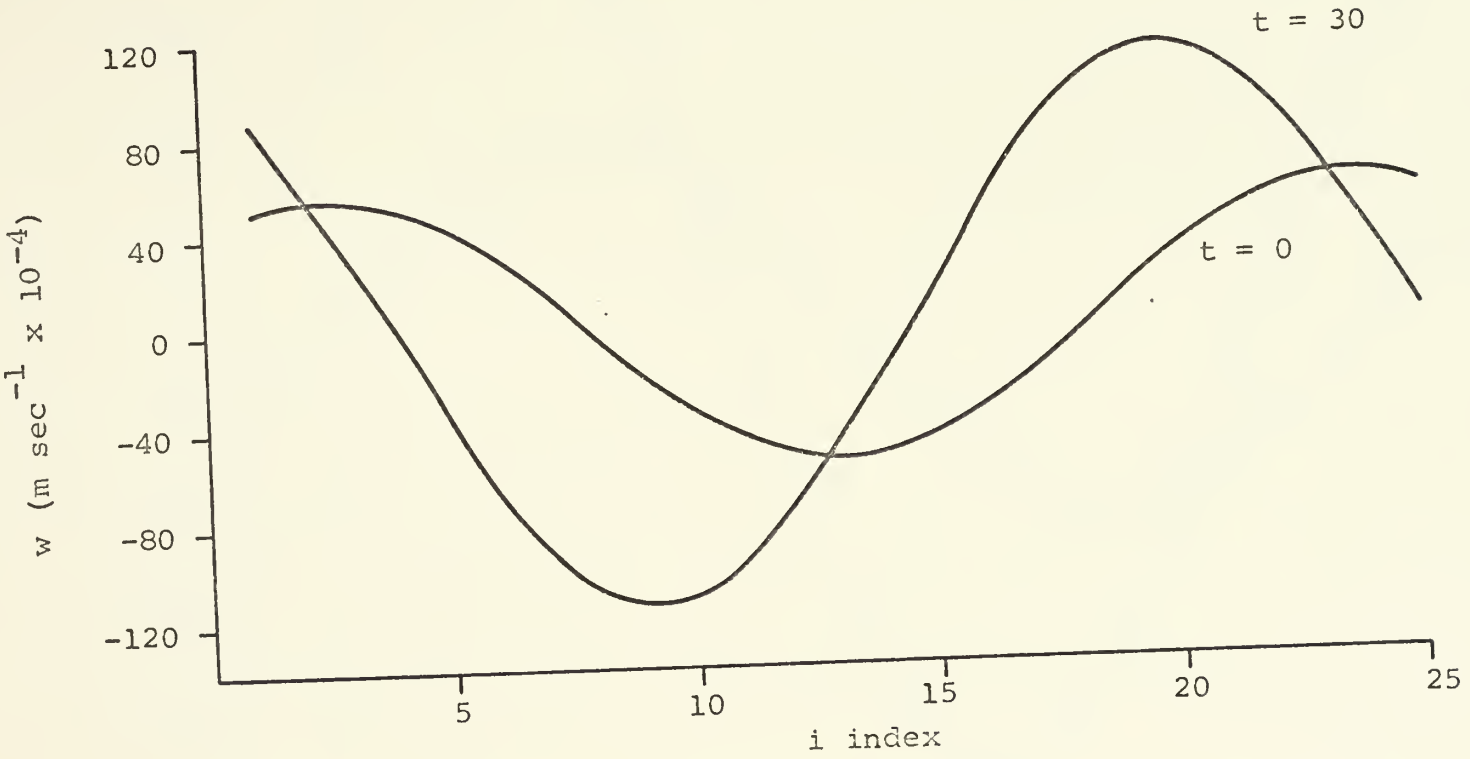

Fig. 2c - The w component of the wave form in the x direction for j=8, k=6, stable case

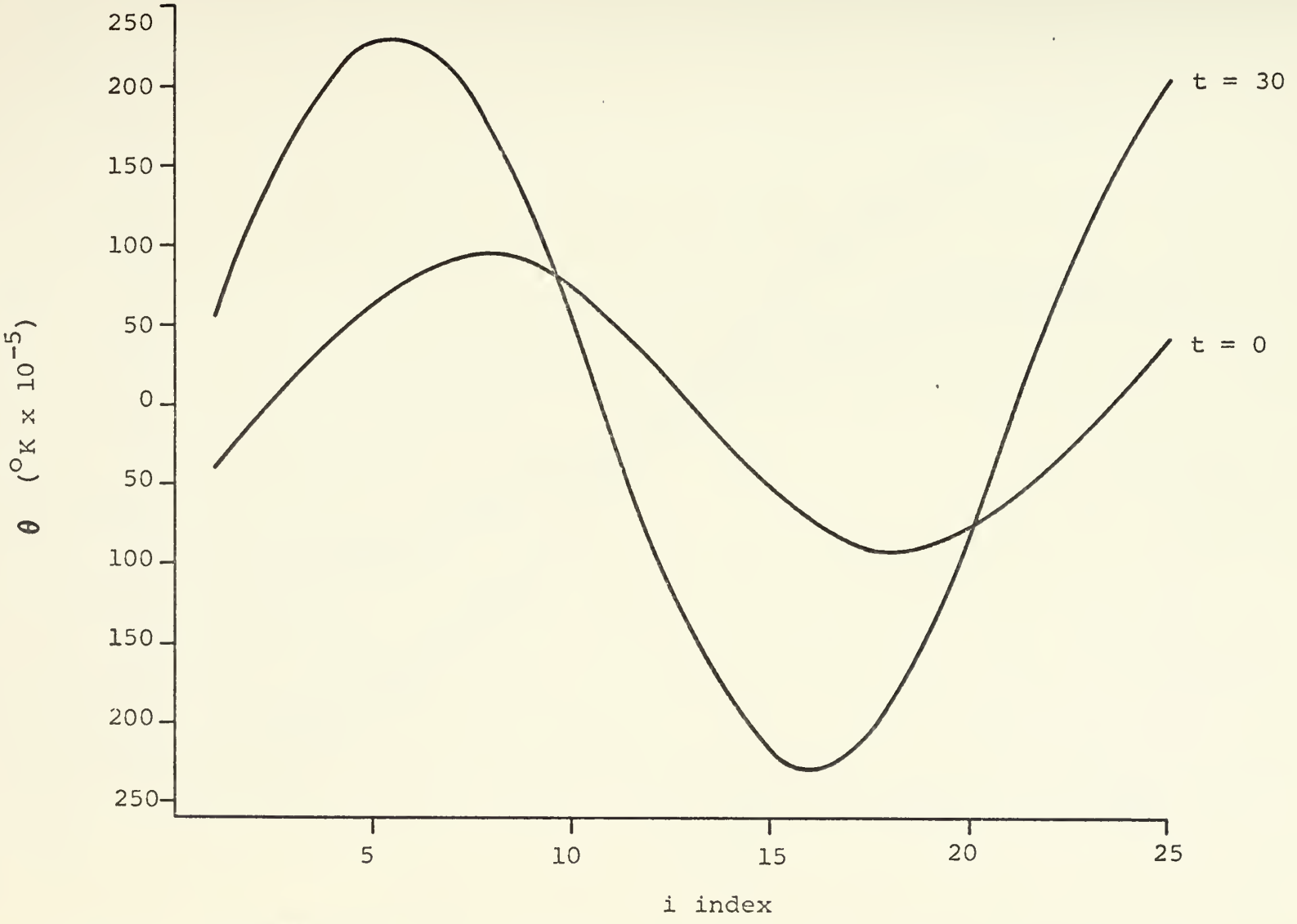

Fig. 2d - The θ wave form in the x direction for j=8, k=6, stable case

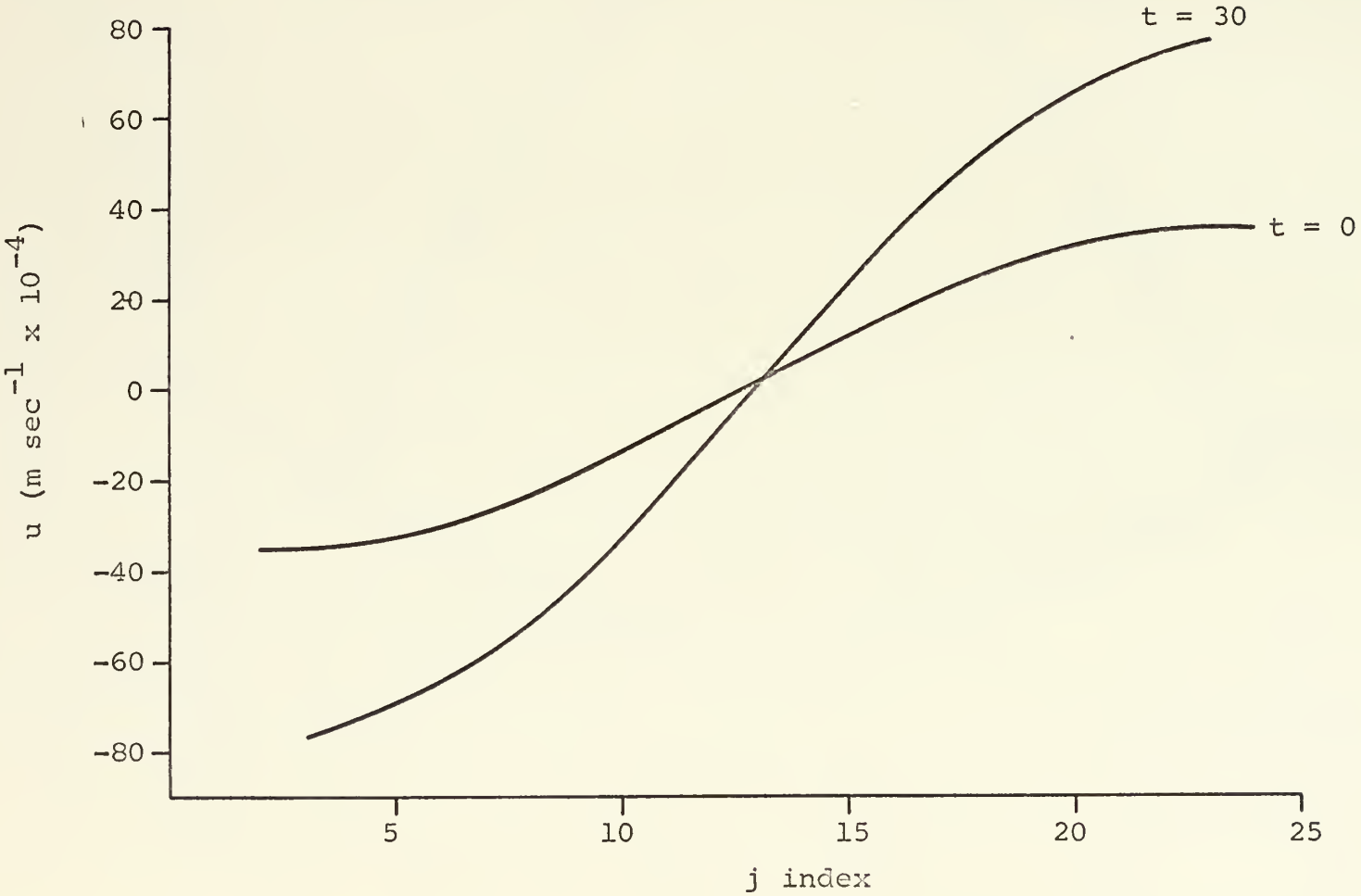

Fig. 3a - The u component of the wave form in the y direction for i=6, k=6, stable case

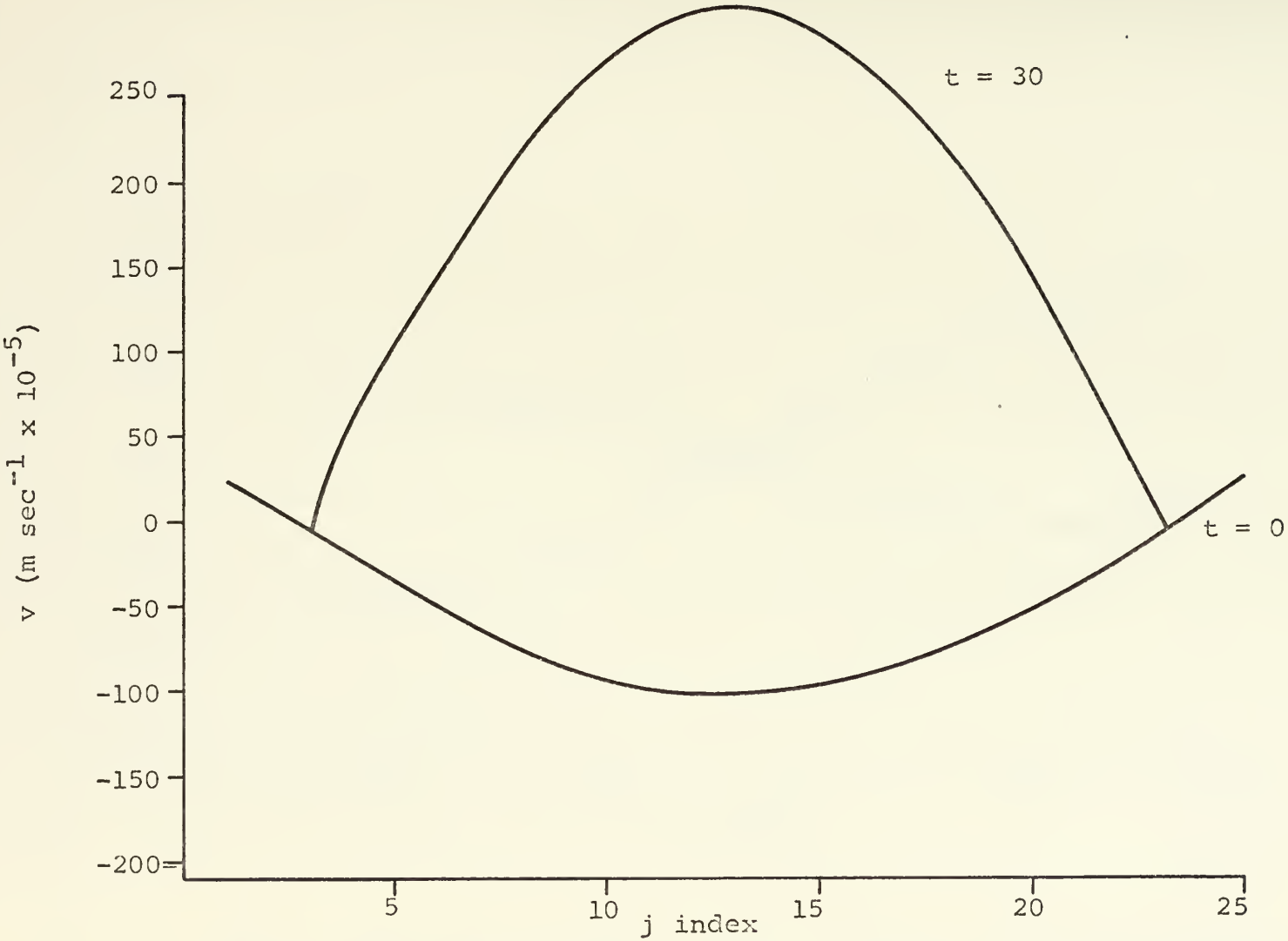

Fig. 3b - The v component of the wave form in the y direction for i=6, k=6, stable case

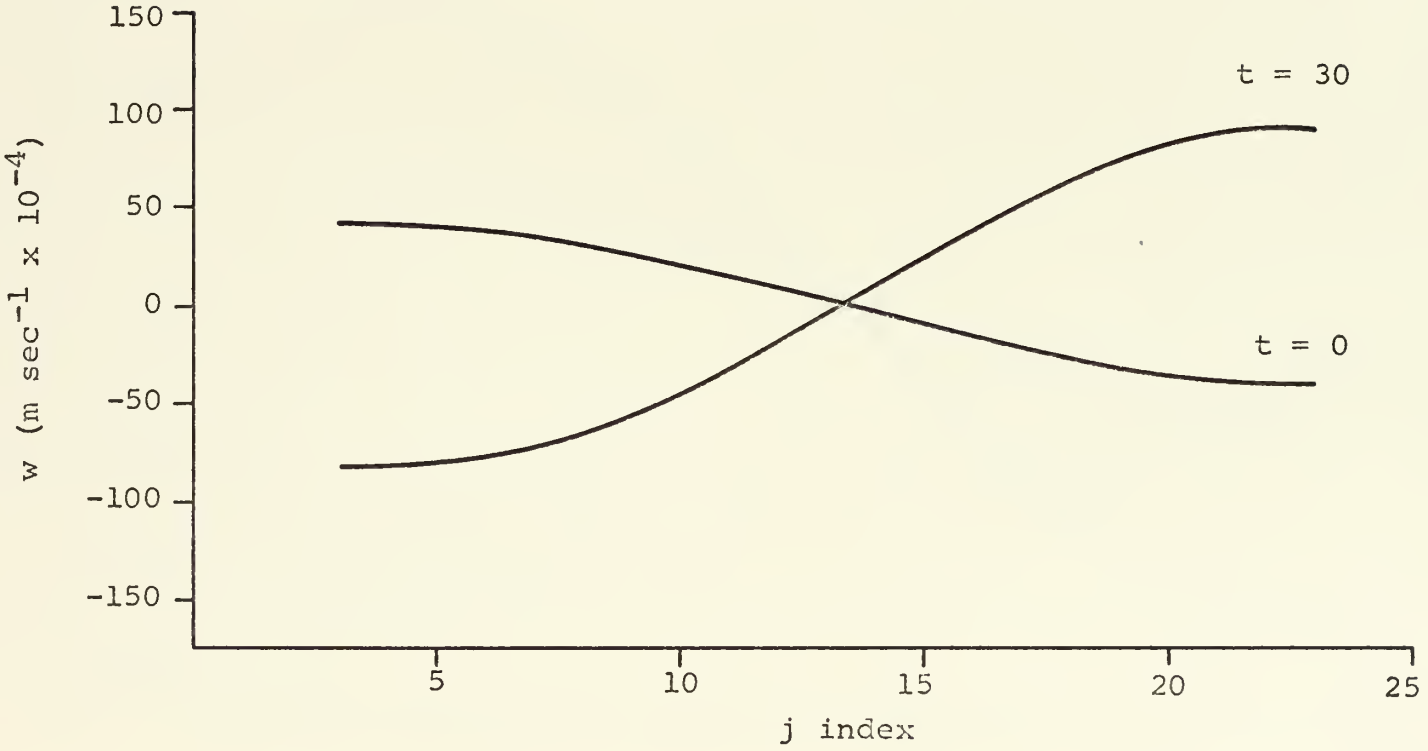

Fig. 3c - The w component of the wave form in the y direction for i=6, k=6, stable case

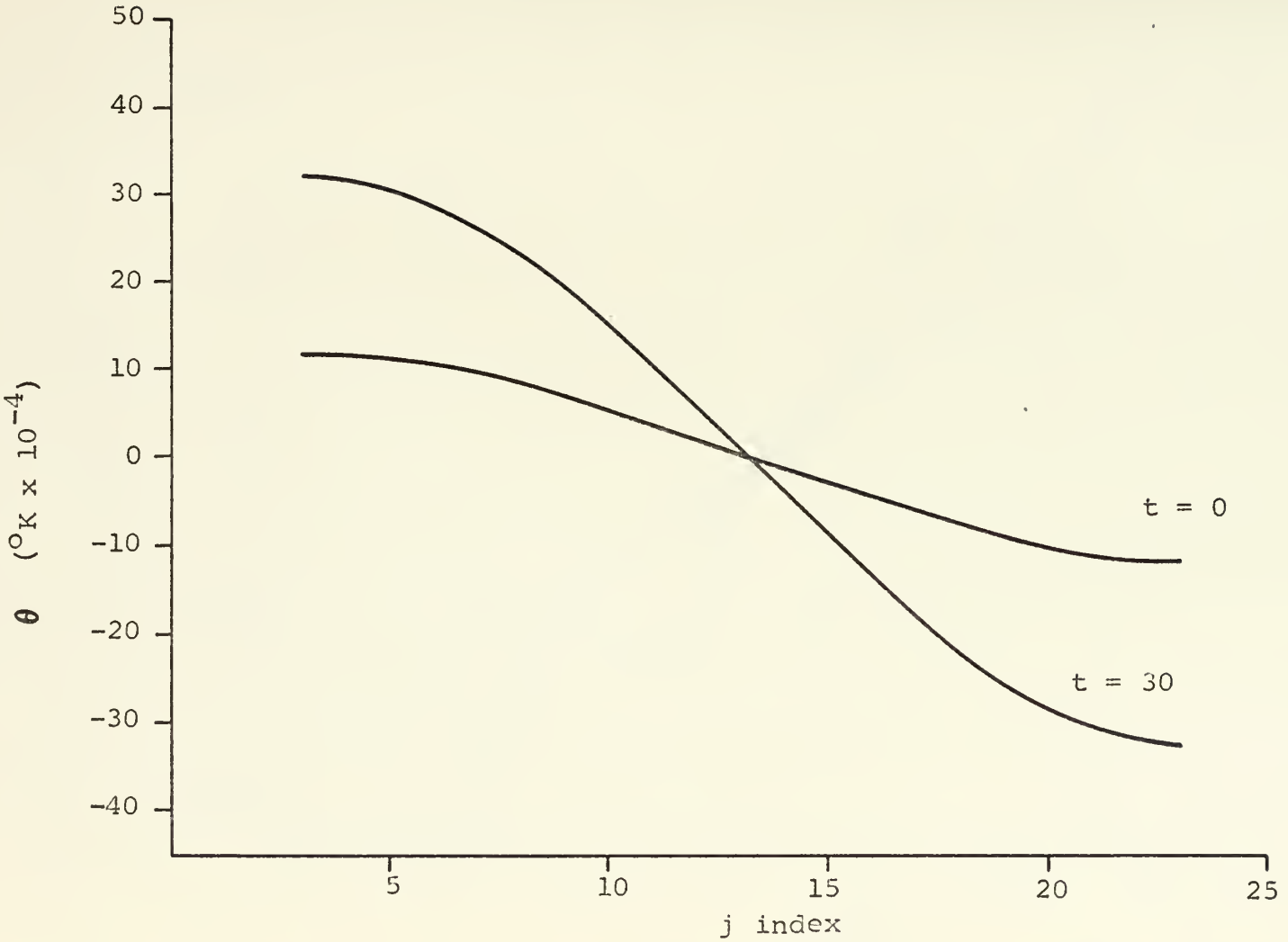

Fig. 3d - The θ wave form in the y direction for i=6, k=6, stable case

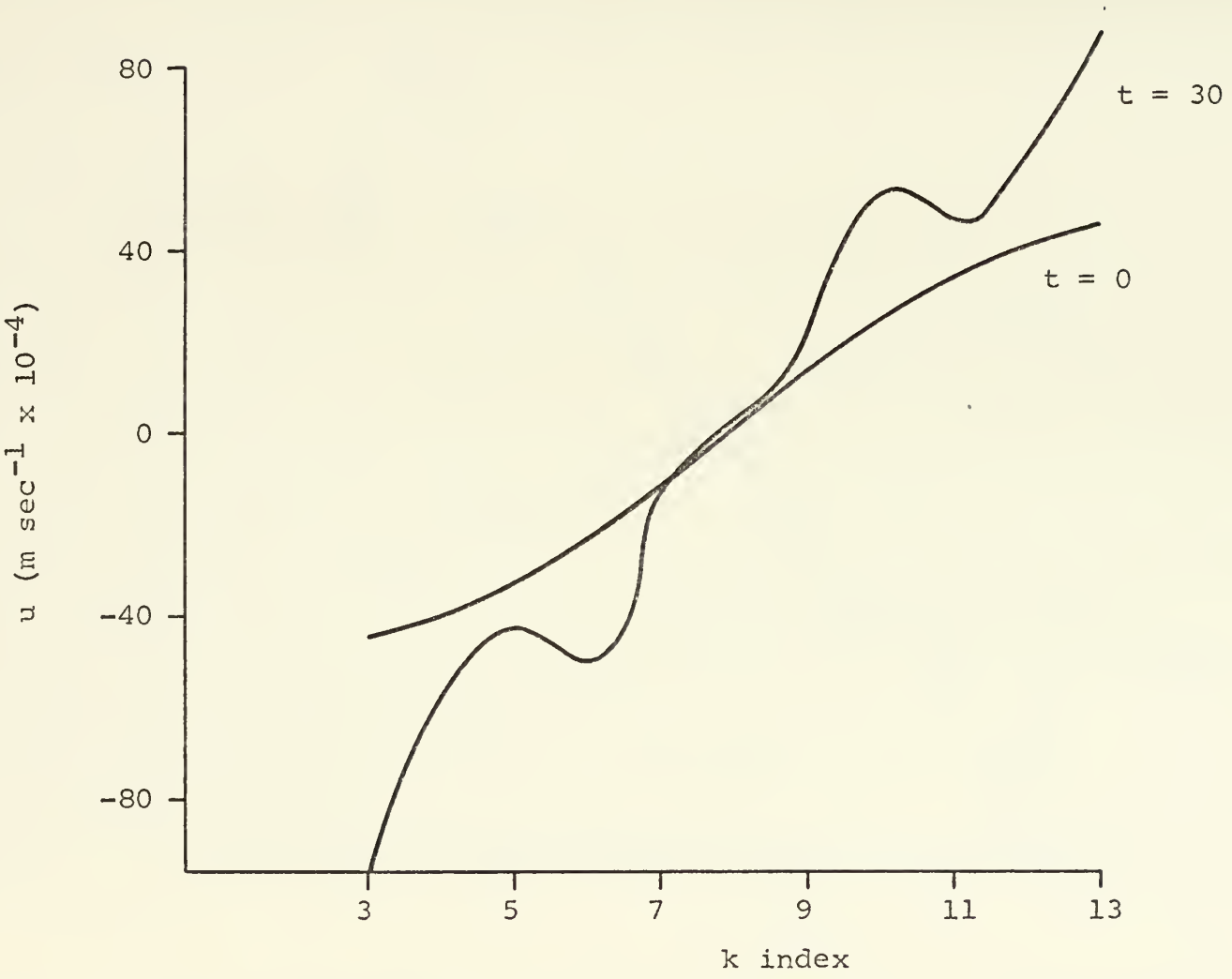

Fig. 4a - The u component of the wave form in the z direction for i=6, j=8, stable case

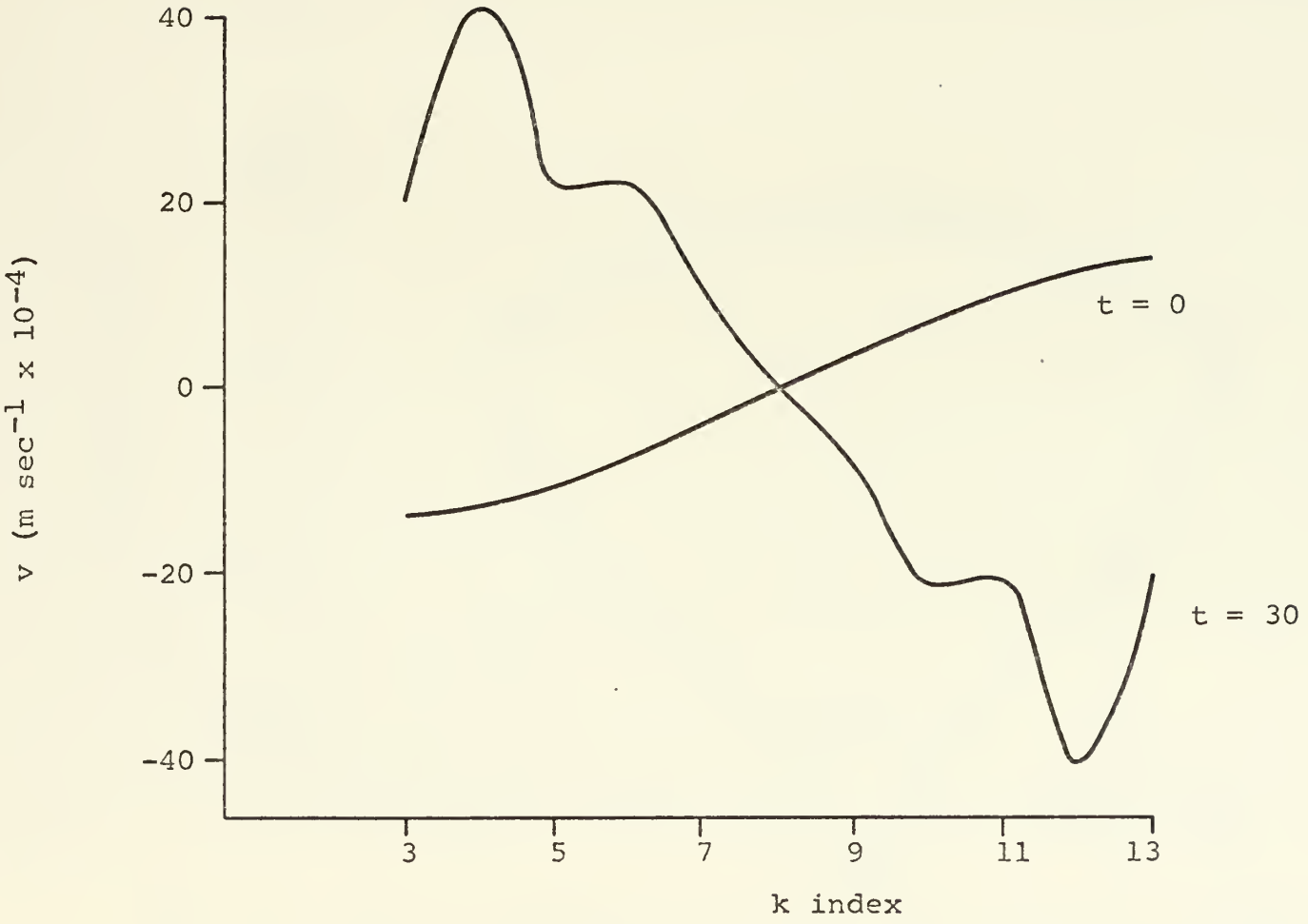

Fig. 4b - The v component of the wave form in the z direction for i=6, j=8, stable case

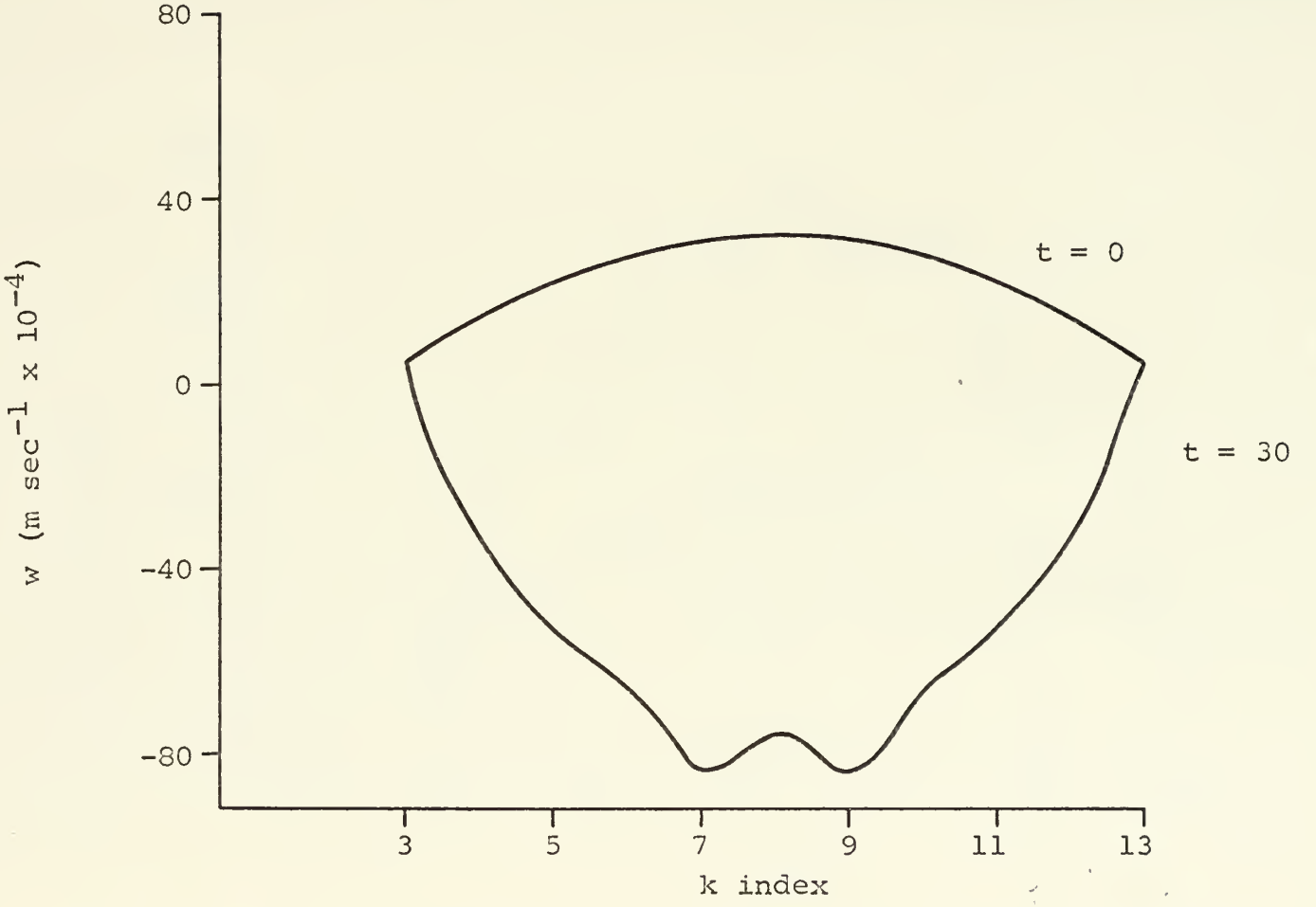

Fig. 4c - The w component of the wave form in the z direction for i=6, j=8, stable case

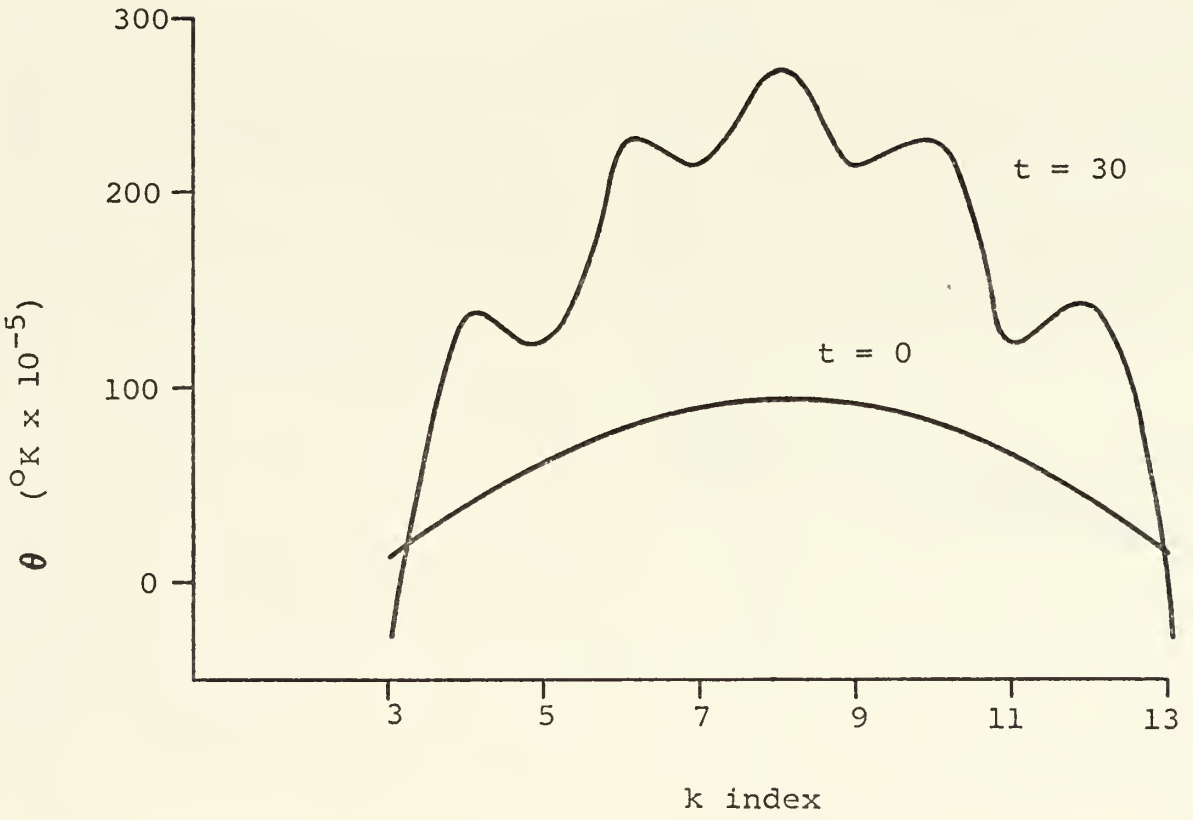

Fig. 4d - The θ wave form in the z direction for i=6, j=8, stable case

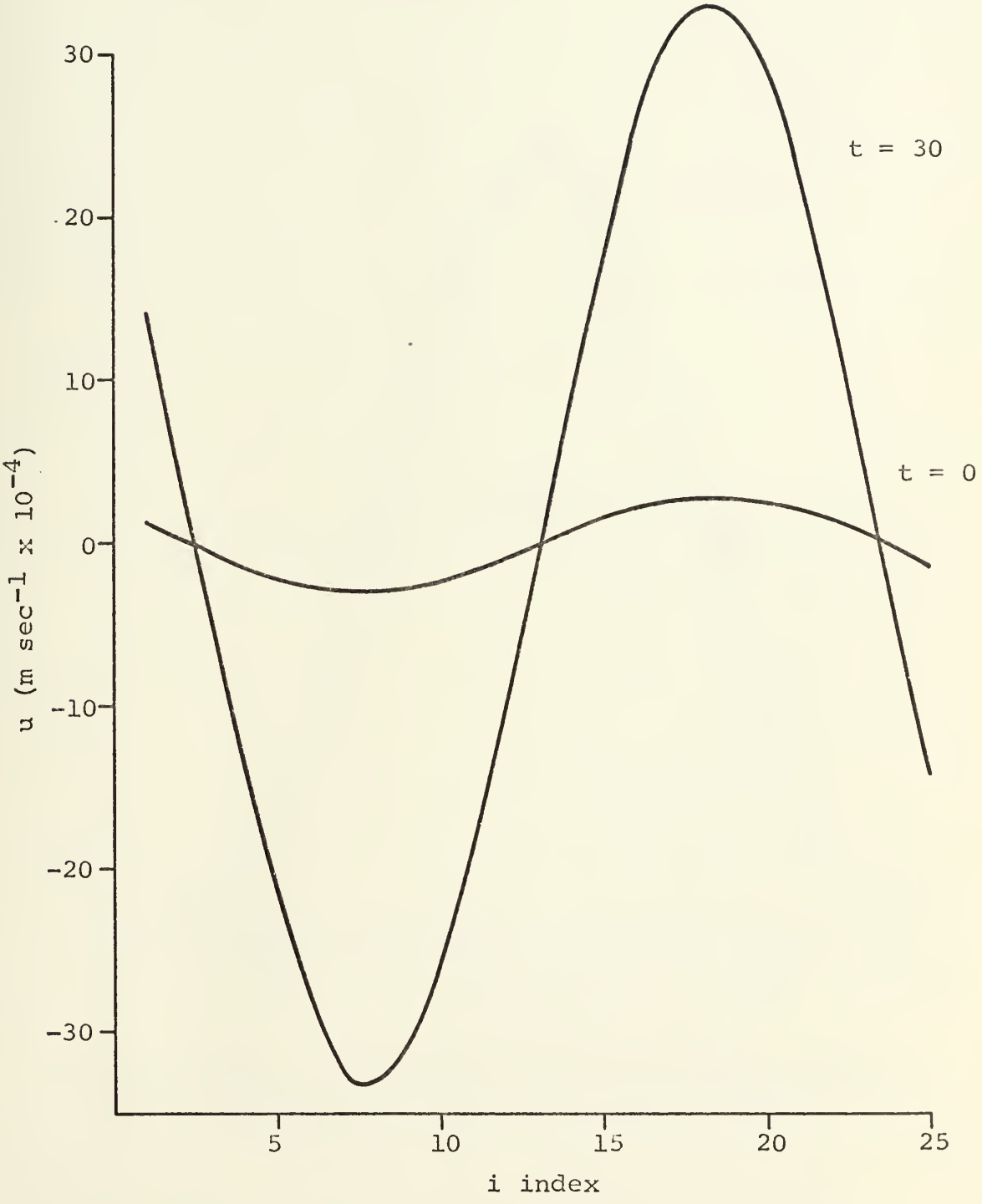

Fig. 5a - The u component of the wave form in the x direction for j=8, k=3, unstable case

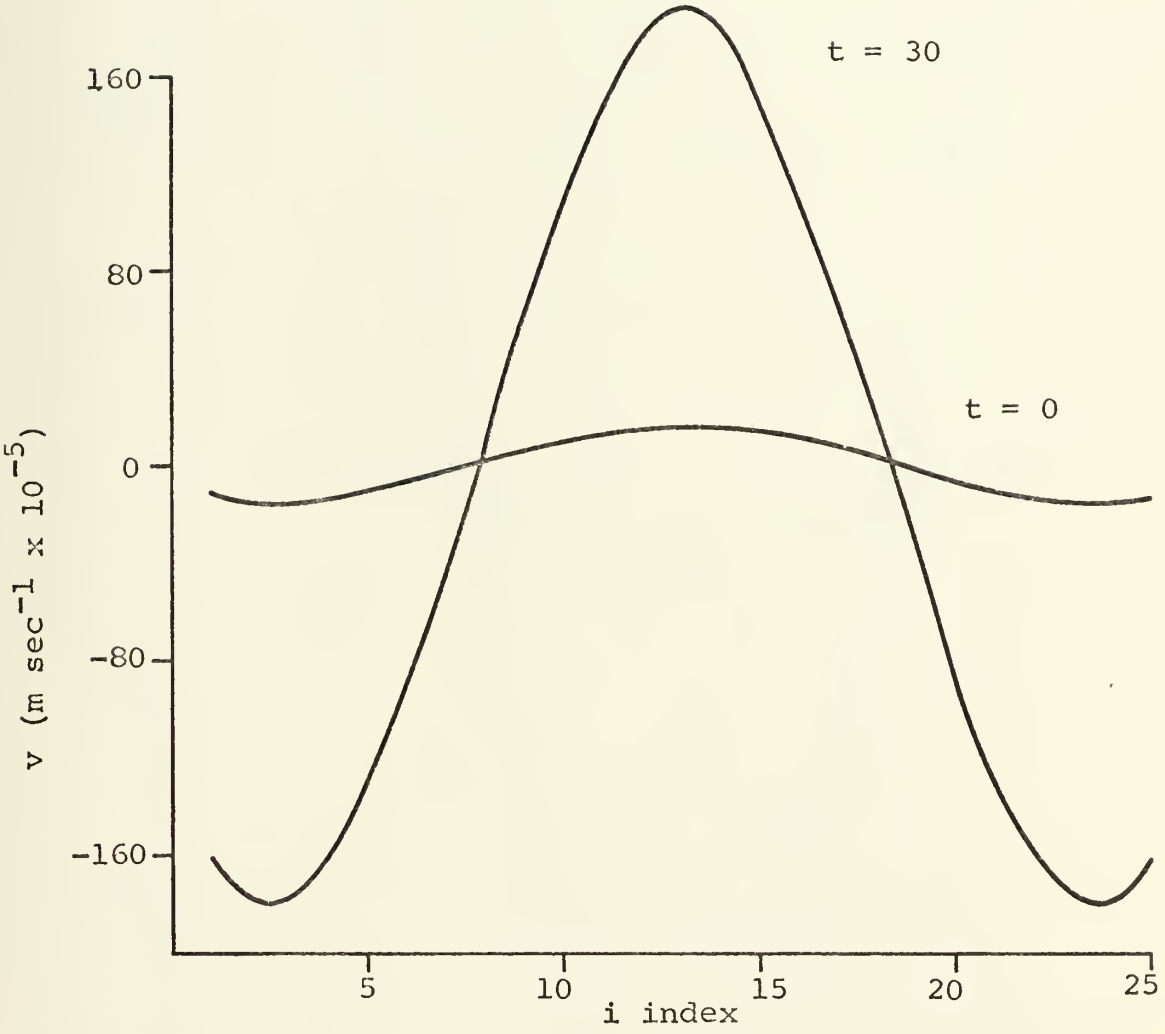

Fig. 5b - The v component of the wave form in the x direction for j=8, k=6, unstable case

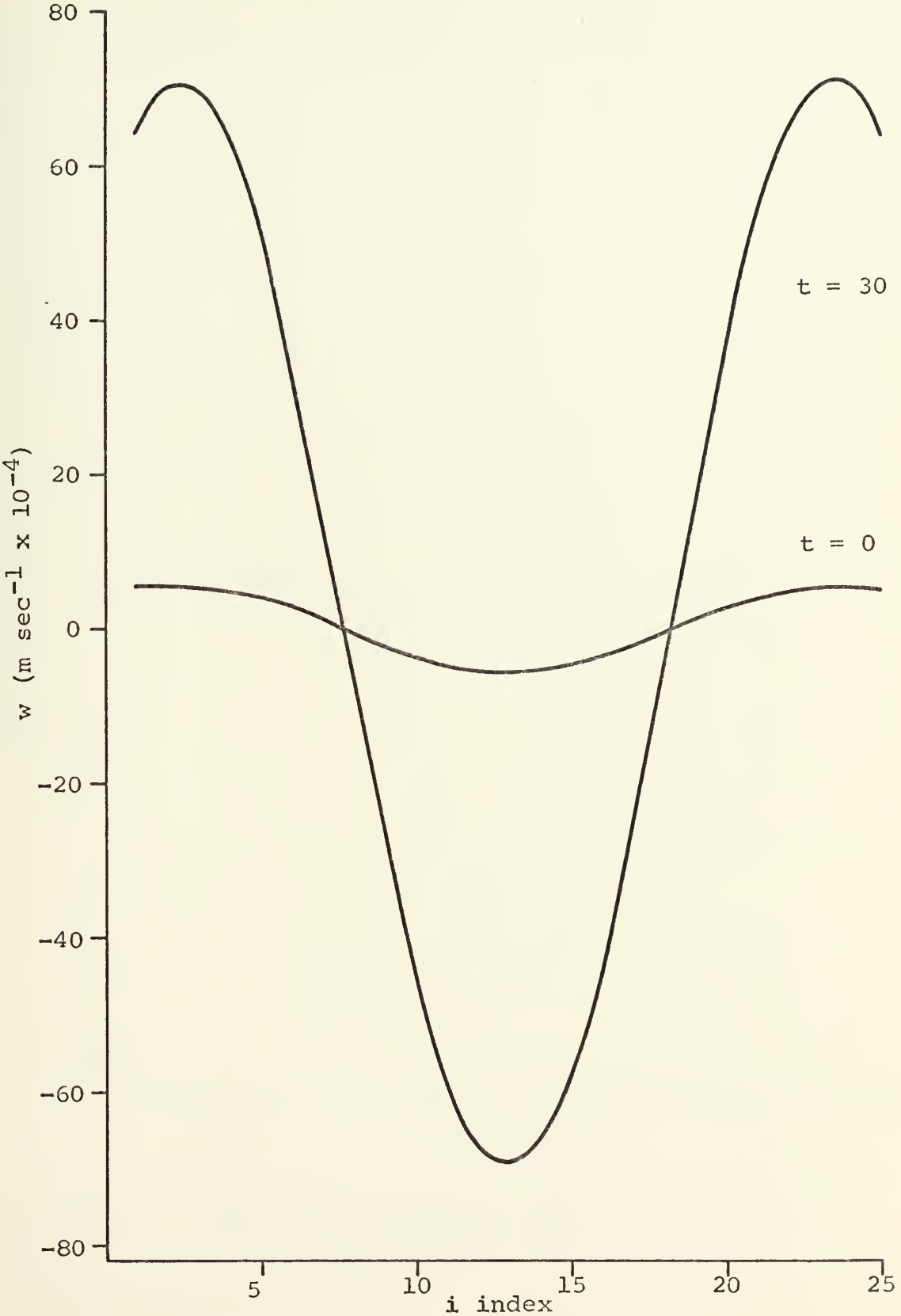

Fig. 5c - The w component of the wave form in the x direction for j=8, k=6, unstable case

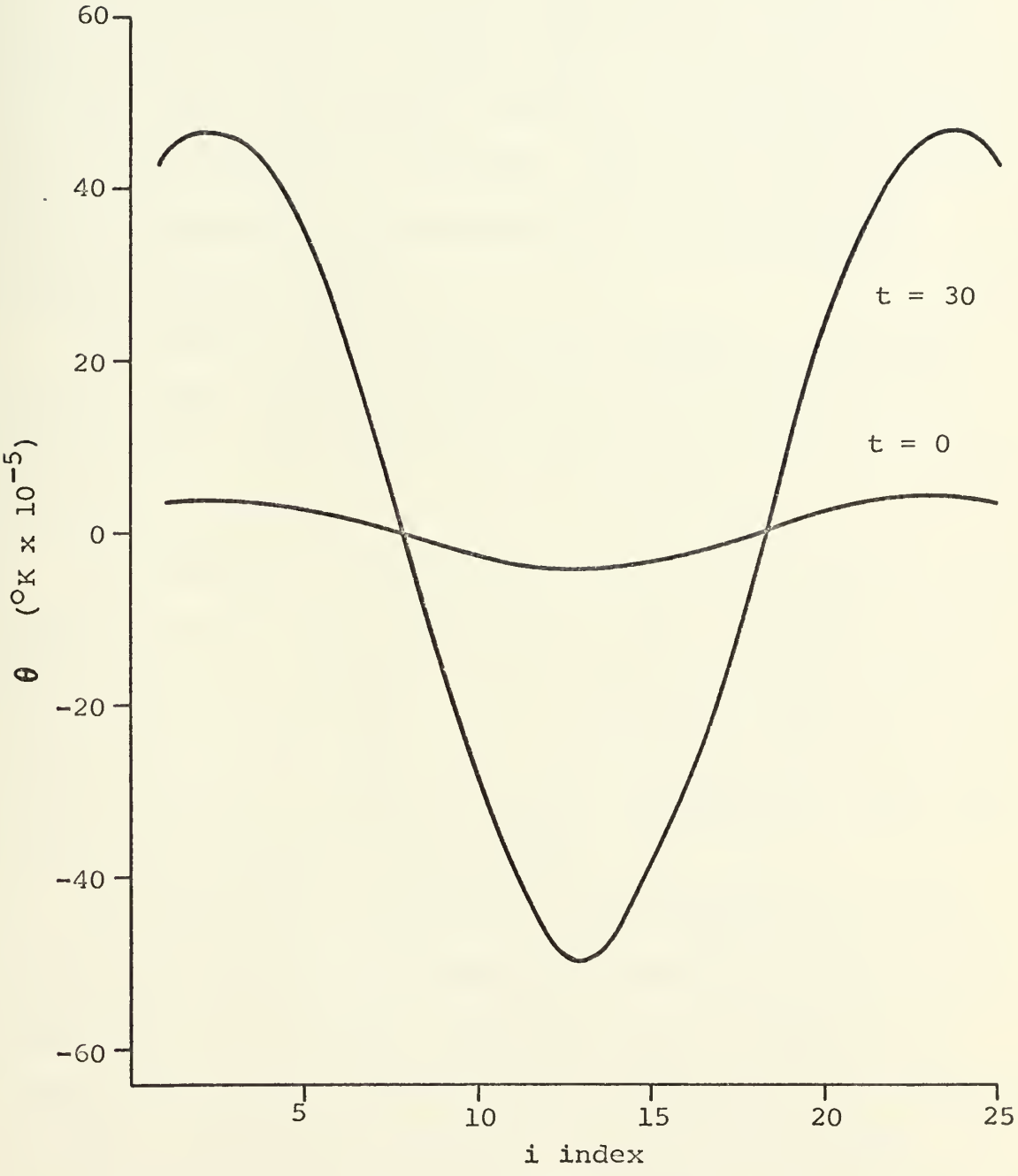

Fig. 5d - The θ wave form in the x direction for j=8, k=6, unstable case

VII. SUMMARY AND CONCLUSIONS

A multi-layer primitive equation model was applied to a mesoscale grid for two test situations. First, a one dimensional, balanced, steady state current was initialized to check the computational stability and finite difference form of the equations of motion. Then an initial gravity wave perturbation was introduced for both stable and unstable stratification.

The stable stratification case yielded a reasonably accurate phase speed of propagation but some undesirable growth of the disturbance was observed, as was discussed in the previous section.

The unstable stratification case produced nearly correct growth rates but some difference in the w and θ growth rates may be an indication that a problem exists similar to that in the stable case, where w and θ waves were propagated at slightly different speeds. Apparently, some small error still exists in the program.

The fact that the growth of the propagating gravity wave can be decreased by inserting a more nearly adiabatic lapse rate of potential temperature can be explained by observing that the buoyancy term in the Boussinesq equations becomes increasingly inaccurate with increased height. By assigning to θ_o a value of potential temperature from a middle level, the error introduced in the buoyancy term is minimized.

Since the Boussinesq equations are accurate only for a shallow atmosphere, the model could be expected to forecast more accurately if the depth were decreased. In such a case the problem with the buoyancy term would be further minimized.

Further studies using this model should have a provision for including vertical compressibility. Additionally, since a primary source of the energy in a thunderstorm-type cloud is latent heat, application to cumulus scale convective activity would be incomplete without the inclusion of moisture.

APPENDIX A

EXTRAPOLATED LIEBMANN RELAXATION SCHEME FOR THREE DIMENSIONAL APPLICATION

The equation to be solved by relaxation is

$$\nabla_3^2 \phi - F = 0 \qquad \text{(A-1)}$$

where

$$F = -\nabla_3 \cdot \left[(\vec{V}_3 \cdot \nabla_3) \vec{V}_3 \right] + f_o \zeta + \frac{g}{\theta_o} \frac{\partial \theta}{\partial z} .$$

Writing (A-1) in finite difference form and expanding yields

$$\frac{\phi_{i+2,j,k} - 2\phi_{i,j,k} + \phi_{i-2,j,k}}{(2\Delta x)^2} +$$

$$\frac{\phi_{i,j+2,k} - 2\phi_{i,j,k} + \phi_{i,j-2,k}}{(2\Delta y)^2}$$

$$+ \frac{\phi_{i,j,k+2} - 2\phi_{i,j,k} + \phi_{i,j,k-2}}{(2\Delta z)^2} - F_{i,j,k} = 0 .$$

Rearranging terms leads to

$$\phi_{i,j,k} = \Big[(2\Delta y)^2 (2\Delta z)^2 (\phi_{i+2,j,k} + \phi_{i-2,j,k})$$

$$+ (2\Delta x)^2 (2\Delta z)^2 (\phi_{i,j+2,k} + \phi_{i,j-2,k})$$

$$+ (2\Delta x)^2 (2\Delta y)^2 (\phi_{i,j,k+2} + \phi_{i,j,k-2})$$

$$- (2\Delta x)^2 (2\Delta y)^2 (2\Delta z)^2 F_{i,j,k} \Big] A$$

where A is the fraction

$$\frac{1}{2\left[(2\Delta y)^2(2\Delta z)^2 + (2\Delta x)^2(2\Delta z)^2 + (2\Delta x)^2(2\Delta y)^2\right]} .$$

Adding and subtracting $\phi^{old}_{i,j,k}$ produces

$$\phi^{new}_{i,j,k} = \phi^{old}_{i,j,k} + A\Big[(2\Delta y)^2(2\Delta z)^2(\phi_{i+2,j,k} + \phi_{i-2,j,k}) + (2\Delta x)^2(2\Delta z)^2(\phi_{i,j+2,k} + \phi_{i,j-2,k}) + (2\Delta x)^2(2\Delta y)^2(\phi_{i,j,k+2} + \phi_{i,j,k-2}) - \frac{\phi^{old}_{i,j,k}}{A} - (2\Delta x)^2(2\Delta y)^2(2\Delta z)^2 F_{i,j,k}\Big] .$$

For successive over relaxation the coefficient α is included, which results in the final form

$$\phi^{new}_{i,j,k} = (1-\alpha)\,\phi^{old}_{i,j,k} + \alpha A\Big[(2\Delta y)^2(2\Delta z)^2(\phi_{i+2,j,k} + \phi_{i-2,j,k}) + (2\Delta x)^2(2\Delta z)^2(\phi_{i,j+2,k} + \phi_{i,j-2,k}) + (2\Delta x)^2(2\Delta y)^2(\phi_{i,j,k+2} + \phi_{i,j,k-2}) - (2\Delta x)^2(2\Delta y)^2(2\Delta z)^2 F_{i,j,k}\Big] \qquad (A\text{-}2)$$

Note that if $\Delta x = \Delta y = \Delta z$, equation (A-2) reduces to the more familiar

$$\phi^{new}_{i,j,k} = (1 - \alpha)\, \phi^{old}_{i,j,k} + \frac{\alpha}{6} \Big[\phi_{i+2,j,k} + \phi_{i-2,j,k} + \phi_{i,j+2,k} + \phi_{i,j-2,k} + \phi_{i,j,k+2} + \phi_{i,j,k-2} - (2\Delta x)^2 F_{i,j,k} \Big] .$$

APPENDIX B

DEVELOPMENT OF THE FORCING FUNCTION

In order to maintain consistent finite differencing between the prognostic equations and the forcing function of the Liebmann relaxation equation, a procedure which was recommended by Dr. R. T. Williams (personal communication) is used to develop the forcing function. The process is carried out in 6 steps for each point in the grid. The 6 steps required to build $F^6_{5,5,5}$, the forcing function at i=5, j=5, k=5, are

$$F^1_{5,5,5} = \frac{-G(w)_{5,5,4}}{2\Delta z}$$

$$F^2_{5,5,5} = \frac{-G(v)_{5,4,5}}{2\Delta y} + F^1_{5,5,5}$$

$$F^3_{5,5,5} = \frac{-G(u)_{4,5,5}}{2\Delta x} + F^2_{5,5,5}$$

$$F^4_{5,5,5} = \frac{G(u)_{6,5,5}}{2\Delta x} + F^3_{5,5,5}$$

$$F^5_{5,5,5} = \frac{G(v)_{5,6,5}}{2\Delta y} + F^4_{5,5,5}$$

$$F^6_{5,5,5} = \frac{G(w)_{5,5,6}}{2\Delta z} + F^5_{5,5,5} ,$$

where

$$G(w) = - \mathfrak{L}(w) + \frac{g\theta}{\theta_o} + \nu \nabla_3^2 w,$$

$$G(v) = - \mathfrak{L}(v) - fu + \nu \nabla_3^2 v,$$

and

$$G(u) = - \mathfrak{L}(u) + fv + \nu \nabla_3^2 u.$$

APPENDIX C

BOUNDARY CONDITIONS AT THE WALLS

For the plane described by j=3, the equations of motion may be written

$$\left(\frac{\partial u}{\partial t}\right)_{i,3,k} = - \mathcal{L}(u)_{i,3,k} - \left(\frac{\partial \Phi}{\partial x}\right)_{i,3,k} + f v_{i,3,k} \qquad \text{(C-1)}$$

$$\left(\frac{\partial v}{\partial t}\right)_{i,3,k} = - \mathcal{L}(v)_{i,3,k} - \left(\frac{\partial \Phi}{\partial y}\right)_{i,3,k} - f u_{i,3,k} \qquad \text{(C-2)}$$

$$\left(\frac{\partial w}{\partial t}\right)_{i,3,k} = - \mathcal{L}(w)_{i,3,k} - \left(\frac{\partial \Phi}{\partial z}\right)_{i,3,k} + \frac{g\,\theta_{i,3,k}}{\theta_o} . \qquad \text{(C-3)}$$

Forming the time derivative of divergence from (C-1), (C-2), and (C-3) and using finite differencing yields

$$0 = \frac{\left(\frac{\partial u}{\partial t}\right)_{i+1,3,k} - \left(\frac{\partial u}{\partial t}\right)_{i-1,3,k}}{2\,\Delta x}$$

$$+ \frac{\left(\frac{\partial v}{\partial t}\right)_{i,4,k} - \left(\frac{\partial v}{\partial t}\right)_{i,2,k}}{2\,\Delta y}$$

$$+ \frac{\left(\frac{\partial w}{\partial t}\right)_{i,j,k+1} - \left(\frac{\partial w}{\partial t}\right)_{i,j,k-1}}{2\,\Delta z} . \qquad \text{(C-4)}$$

Introducing the condition (C-5)

$$v_{i,2,k} = - v_{i,3,k} ,$$

which implies

$$\frac{\partial v}{\partial t}_{i,2,k} = - \frac{\partial v}{\partial t}_{i,3,k} ,$$

(C-4) becomes

$$0 = \frac{\frac{\partial u}{\partial t}_{i+1,3,k} - \frac{\partial u}{\partial t}_{i-1,3,k}}{2\Delta x} + \frac{\frac{\partial v}{\partial t}_{i,4,k} + \frac{\partial v}{\partial t}_{i,3,k}}{2\Delta y} + \frac{\frac{\partial w}{\partial t}_{i,3,k+1} - \frac{\partial w}{\partial t}_{i,3,k-1}}{2\Delta z} \qquad (C-6)$$

Expansion of (C-6) yields

$$\nabla^2 \Phi_{i,3,k} = \frac{- \Phi_{i,3,k} + \Phi_{i,1,k} - \Phi_{i,4,k} + \Phi_{i,2,k}}{(2\Delta y)^2} - \frac{\mathfrak{L}(u)_{i+1,3,k} - \mathfrak{L}(u)_{i-1,3,k}}{2\Delta x} - \frac{\mathfrak{L}(v)_{i,4,k} + \mathfrak{L}(v)_{i,3,k}}{2\Delta y} - \frac{\mathfrak{L}(w)_{i,3,k+1} - \mathfrak{L}(w)_{i,3,k-1}}{2\Delta z} + \frac{f(v_{i+1,3,k} - v_{i-1,3,k})}{2\Delta x} - \frac{f(u_{i,4,k} + u_{i,3,k})}{2\Delta y} + \frac{g(\theta_{i,3,k+1} - \theta_{i,3,k-1})}{2\Delta z\, \theta_o} . \qquad (C-7)$$

Applying the conditions

$$u_{i,2,k} = u_{i,3,k} \quad , \tag{C-8}$$

$$\phi_{i,3,k} - \phi_{i,1,k} = -2\,\Delta yfu_{i,2,k} \quad , \tag{C-9}$$

and

$$\phi_{i,4,k} - \phi_{i,2,k} = -2\,\Delta yfu_{i,3,k} \quad , \tag{C-10}$$

produces

$$\nabla^2 \phi_{i,3,k} = F_{i,3,k} \quad ,$$

which is the equation to be solved by relaxation.

Thus, the conditions for the southern boundary must include the relationships given by (C-5), (C-8), (C-9) and (C-10).

A similar approach produces corresponding conditions at the northern boundary. These conditions are

$$v_{i,JM-1,k} = - v_{i,JM-2,k} \quad , \tag{C-11}$$

$$u_{i,JM-1,k} = u_{i,JM-2,k} \quad , \tag{C-12}$$

$$\phi_{i,JM,k} - \phi_{i,JM-2,k} = -2\,\Delta yf\, u_{i,JM-1,k} \quad , \tag{C-13}$$

and

$$\phi_{i,JM-1,k} - \phi_{i,JM-3,k} = -2\,\Delta yf\, u_{i,JM-2,k} \quad . \tag{C-14}$$

For the plane described by k=3, the same process can be carried out to develop boundary conditions at the top and bottom, which are

$$w_{i,j,2} = -w_{i,j,3} \quad , \tag{C-15}$$

$$\Phi_{i,j,3} - \Phi_{i,j,1} = \frac{2\Delta zg}{\theta_o} \theta_{i,j,2} \quad , \tag{C-16}$$

$$\Phi_{i,j,4} - \Phi_{i,j,2} = \frac{2\Delta zg}{\theta_o} \theta_{i,j,3} \quad , \tag{C-17}$$

$$w_{i,j,KM-1} = -w_{i,j,KM-2} \quad , \tag{C-18}$$

$$\Phi_{i,j,KM} - \Phi_{i,j,KM-2} = \frac{2\Delta zg}{\theta_o} \theta_{i,j,KM-1} \tag{C-19}$$

and

$$\Phi_{i,j,KM-1} - \Phi_{i,j,KM-3} = \frac{2\Delta zg}{\theta_o} \theta_{i,j,KM-2} \quad . \tag{C-20}$$

LIST OF REFERENCES

1. Arakawa, A., 1962: Non-geostrophic effects in the baroclinic prognostic equations. Proc. Intern. Symp. Numerical Weather Prediction, Tokyo, 161-175.

2. Browning, K. A., 1964: Airflow and precipitation trajectories within severe local storms which travel to the right of the winds. J. Atmos. Sci., 21, 634-639.

3. Deardorff, J. W., 1970: A numerical study of three-dimensional turbulent channel flow at large Reynolds numbers. J. Fluid Mech., 41, 453-480.

4. Fankhauser, J. C., 1968: Thunderstorm-environment interactions revealed by chaff trajectories in the mid-troposphere. Tech. Mem. IERTM-NSSL 39, 14 pp.

5. Lilly, D. K., 1962: On the numerical simulation of buoyant convection. Tellus, 14, 148-172.

6. Newton, C. W., 1966: Circulations in large sheared cumulonimbus. Tellus, 18, 699-713.

7. Newton, C. W., and H. R. Newton, 1959: Dynamical interactions between large convective clouds and environment with vertical shear. J. Meteor., 16, 483-496.

8. Normand, C. W. B., 1946: Energy in the atmosphere. Quart. J. R. Meteor., 18, 451-467.

9. Ogura, Y., 1963: A review of numerical modeling research on small scale convection in the atmosphere. Meteorological Monographs, 5, 65-76.

10. Ogura, Y., and N. A. Phillips, 1962: Scale analysis of deep and shallow convection in the atmosphere. J. Atmos. Sci., 19, 173-179.

INITIAL DISTRIBUTION LIST

		No. Copies
1.	Library Naval Postgraduate School Monterey, California 93940	2
2.	Defense Documentation Center Cameron Station Alexandria, Virginia 22314	2
3.	Asst. Professor R. L. Alberty, Code 51 AL Department of Meteorology Naval Postgraduate School Monterey, California 93940	5
4.	Professor G. J. Haltiner, Department Chairman Department of Meteorology Naval Postgraduate School Monterey, California 93940	1
5.	Assoc. Professor R. T. Williams, Code 51 Wu Department of Meteorology Naval Postgraduate School Monterey, California 93940	1
6.	Department of Meteorology Code 51 Naval Postgraduate School Monterey, California 93940	2
7.	Asst. Professor R. L. Elsberry, Code 51 Es Department of Meteorology Naval Postgraduate School Monterey, California 93940	1
8.	LTCDR Jack T. Norton, Jr. U. S. Fleet Weather Central Norfolk, Virginia 23511	2
9.	Dr. A. Arakawa Department of Meteorology U. C. L. A. Los Angeles, California 90024	1

DOCUMENT CONTROL DATA - R & D

(Security classification of title, body of abstract and indexing annotation must be entered when the overall report is classified)

1 ORIGINATING ACTIVITY (Corporate author)

Naval Postgraduate School
Monterey, California 93940

2a. REPORT SECURITY CLASSIFICATION
Unclassified

2b. GROUP

3 REPORT TITLE

A Three Dimensional Primitive Equation Model for Application to Mesoscale Atmospheric Phenomena

4 DESCRIPTIVE NOTES (Type of report and inclusive dates)
Master's Thesis; September 1970

5. AUTHOR(S) (First name, middle initial, last name)

Jack Trask Norton, Jr.

6. REPORT DATE	7a. TOTAL NO. OF PAGES	7b. NO. OF REFS
September 1970	58	9

8a. CONTRACT OR GRANT NO

b. PROJECT NO

c.

d.

9a. ORIGINATOR'S REPORT NUMBER(S)

9b. OTHER REPORT NO(S) (Any other numbers that may be assigned this report)

10 DISTRIBUTION STATEMENT

This document has been approved for public release and sale; its distribution is unlimited.

11. SUPPLEMENTARY NOTES

12. SPONSORING MILITARY ACTIVITY

Naval Postgraduate School
Monterey, California 93940

13 ABSTRACT

A three dimensional primitive equation model based on the Boussinesq equations is developed and applied to the mesoscale. The model is tested with one dimensional flow in a balanced state and with two cases of gravity waves, which are forecast for 30 minutes and compared with the analytic solutions.

DD FORM 1 NOV 68 1473 (PAGE 1)
S/N 0101-807-6811

Unclassified
Security Classification

A-31408

14 KEY WORDS	LINK A		LINK B		LINK C	
	ROLE	WT	ROLE	WT	ROLE	WT
BOUSSINESQ EQUATIONS						
MESOSCALE GRID						
THREE DIMENSIONAL PRIMITIVE EQUATION MODEL						

Thesis 122751
N942 Norton
c.1 A three dimensional primitive equation model for application to mesoscale atmospheric phenomena.

122751
Thesis
N942 Norton
c.1 A three dimensional primitive equation model for application to mesoscale atmospheric phenomena.

thesN942
A three dimensional primitive equation m
3 2768 001 94745 0
DUDLEY KNOX LIBRARY